

# Fine-Tune Language Models as Multi-Modal Differential Equation Solvers

Liu Yang, Siting Liu, Stanley J. Osher\*

Department of Mathematics, UCLA, Los Angeles, CA 90095, USA

In the growing domain of scientific machine learning, in-context operator learning [1] has shown notable potential in learning operators and solving differential equations using prompted data, during the inference stage without weight updates. However, the current model’s overdependence on function data, may inadvertently overlook the invaluable human insight into the operator. To address this, we present a transformation of in-context operator learning into a multi-modal paradigm. In particular, we take inspiration from the recent success of large language models, and propose using “captions” to integrate human knowledge about the operator, expressed through natural language descriptions and equations. Also, we introduce a novel approach to train a language-model-like architecture, or directly fine-tune existing language models, for in-context operator learning. We beat the baseline on single-modal learning tasks, and also demonstrated the effectiveness of multi-modal learning in enhancing performance and reducing function data requirements. The proposed method not only significantly improves in-context operator learning, but also creates a new path for the application of language models.

## 1 Introduction

In [1], the authors introduced in-context operator learning as a new paradigm for operator learning. As in classic operator learning tasks, an operator maps a single input function or a tuple of input functions, referred to as the “condition”, to an output function, referred to as the “quantity of interest (QoI)”. In practice, we usually have no access to the analytical expression of these functions, but instead can collect function data in the form of key-value pairs, where the keys are discrete function inputs and the values are the corresponding function outputs.

A wide variety of scientific machine learning tasks can be conceptualized as operator learning problems. Consider the task of solving partial differential equations (PDEs) for instance, where the coefficient function serves as the

---

\*Corresponding Author: [sjo@math.ucla.edu](mailto:sjo@math.ucla.edu).

See code in <https://github.com/LiuYangMage/in-context-operator-networks>

condition, and the solution is the QoI. Conversely, for inverse problems, these roles are swapped. When dealing with problems involving temporal evolution, the condition can be the initial function, while the QoI represents the function at a later time. For control problems, the condition could correspond to the cost function and the initial state, while the QoI embodies the control signal. It’s evident that the relationship between the condition and the QoI is highly contingent on the operator, which diverges based on the task at hand and the particular system in question.

In classic operator learning approaches [2, 3, 4, 5, 6, 7, 8, 9, 10, 11, 12], the neural networks are limited to approximate specific operators, and thus need to be trained every time a new operator is encountered. In contrast, in-context operator learning aims to train the model as an “operator learner” instead of an “operator approximator”. In particular, the model is trained to learn the operator from the prompted condition-QoI pairs, referred to as “examples”, and apply the learned operator to the question condition to predict the corresponding QoI. After training, the above learning process can be performed in the inference stage without weight update. This approach offers a “train-once-apply-multiple” paradigm and paves the way for large-scale foundation models [13] for a broad array of scientific machine learning tasks.

The study by [1] showcases the successful implementation of in-context operator learning, which relies solely on function data. However, a crucial aspect of scientific machine learning is overlooked in this approach, namely, the human knowledge of the operator, which can span from nebulous natural language explanations to explicit differential equations. There’s a strong case for incorporating such knowledge into the learning system alongside function data, as this could potentially enhance learning performance. If the human understanding of the operator is sufficiently detailed, the system might require fewer examples to learn the operator. Theoretically, it might even enable zero-shot learning, where the operator could be learned and utilized without the need for any examples.

Past research on the topic of scientific machine learning typically integrates human knowledge into the learning system by designing special loss functions or neural network architectures based on the differential equations or symmetry/conservation laws that govern the system. While these approaches have witnessed significant success, they are not without limitations. Firstly, it may not always be practical to design special loss functions or architectures, as the system might not be fully understood by humans, or the operator might be too complicated to be described by equations. Secondly, these bespoke loss functions or architectures are tailored for specific systems or tasks. When confronted with a new system, there is a requirement not only to design new loss functions or architectures but also typically to retrain the neural network.

In this paper, we explore an entirely different approach to infusing human knowledge into the learning system. Inspired by the recent success of large language models, we introduce a new component to in-context operator learning: the “caption”. A caption is a string serving as a descriptor of the operator, and can take various forms such as equations written in LaTeX forms, natural language descriptions, or a combination of both. Rather than crafting special loss

functions or architectures, we simply feed the caption into the neural network as input alongside the examples. We thus evolve the in-context operator learning to be multi-modal, meaning that the neural network can learn the operator from function data, captions, or a combination of both. The diagram in Figure 1 illustrates the multi-modal in-context operator learning.

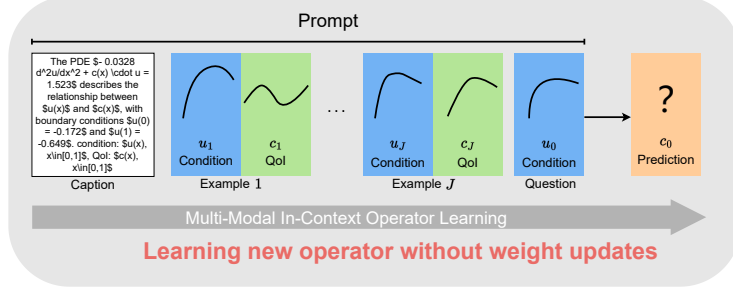


Figure 1: Diagram for multi-modal in-context operator learning.

This method is substantially more flexible and can accommodate a broader range of systems under the same framework. Moreover, it retains the principle of in-context operator learning, where human knowledge is integrated into the learning system without any weight update.

We also introduce a novel approach to train a language-model-like architecture, or directly fine-tune existing language models, for in-context operator learning. We inherit the transformer and word embedding layers from language models, and also mimic the “next-token prediction” training scheme so that the model predicts the QoI in each example based on preceding examples. The main deviation (and also the key challenge) is the necessity to design the input sequence and formulate a specialized mask to accommodate in-context operator learning tasks. Following the name “In-Context Operator Networks (ICON)” introduced in [1], we refer to our architecture and training scheme as “ICON-LM”, where “LM” stands for “language model”.

The adoption of language models for in-context learning is crucial for two reasons. First, it enables us to utilize existing techniques and tools developed for language models for in-context operator learning. Second, it paves the way to broaden the capability of language models to scientific machine learning tasks with heavy numerical computations, which is a weak spot in the current ecosystem of language models.

In our experiments, by training a language-model-like architecture from scratch, we beat the original “ICON” in terms of accuracy on single-modal tasks, with less training time, comparable memory requirement, and about half the number of parameters. We also fine-tuned the GPT-2 model to demonstrate the effectiveness of multi-modal learning in enhancing performance and reducing function data requirements. Notably, given the absence of multi-modal datasets for in-context operator learning with language captions (as far as we’re aware), we augmented the single-modal dataset from [1] with caption data, leveraging

the capabilities of the GPT-4 API. We hope this dataset can serve as a benchmark for future research on multi-modal in-context operator learning.

Our contributions are summarized as follows:

1. We transform the in-context operator learning into a multi-modal framework by introducing “captions” as a means to incorporate human knowledge about the operator, in the form of natural language descriptions and equations.
2. We introduce a novel approach, namely “ICON-LM”, to train a language-model-like architecture, or directly fine-tune existing language models, for in-context operator learning. We beat the baseline on single-modal learning tasks, and also demonstrated the effectiveness of multi-modality with ICON-LM in enhancing performance and reducing function data requirements.
3. Leveraging the capabilities of the GPT-4 API, we generated a multi-modal dataset for in-context operator learning with language captions, which aims to serve as a benchmark for future research in this area.
4. By bridging language models with operator learning and data-driven differential equation solvers, we have not only achieved substantial advancements in this specific domain, but also opened up a new avenue for the application of language models in scientific machine learning, especially in areas that require heavy numerical computations, such as solving differential equations, a realm that remains largely under-explored.

The rest of the paper is organized as follows. In Section 2, we review the related work. In Section 3, we show the caption data generation. In Section 4, we introduce the ICON-LM architecture and training scheme. In Section 5, we present the experimental results. Finally, we conclude in Section 6.

## 2 Related Work

### 2.1 Operator Learning and In-Context Operator Learning

Numerous neural network methods have been proposed for approximating operators, i.e., mappings that take functions as input and output. The early works of [2, 3] employed shallow neural networks for the approximation of nonlinear operators. A deep neural network approach to tackle parametric PDE challenges was suggested in [4]. PDE-Net, as presented in [6] enables forward predictions of PDE solutions using the inferred forward map. The study in [5] presented a Bayesian method to address uncertainty quantification in stochastic PDE scenarios. The Deep Operator Network (DeepONet), referenced in [7], introduces a neural network design that approximates the solution operator, mapping parameters or initial/boundary conditions to their corresponding solutions. The

Fourier Neural Operator (FNO) from [9, 10] leverages the Fourier space’s integral kernel to approximate the solution operator. Drawing inspiration from neural networks and model reduction, the paper [11] estimates input-output maps between infinite-dimensional spaces for parametric PDEs. Additional contributions can be found in [14, 15, 16, 17, 18].

Recently, a different operator learning paradigm, namely in-context operator learning, is proposed in [1]. Instead of approximating specific operators, in-context operator learning trains the neural network as an operator learner, which can learn and apply the operator in the inference stage without weight update.

## 2.2 Physics-Informed Machine Learning

In the literature, two approaches are commonly employed to incorporate physical knowledge in neural networks: hard constraints and soft constraints. We refer readers to the survey paper [19] on this topic. Hard constraints involve designing neural network architectures in a way that ensures any solution generated by the network meets the specified constraints (see, for example, [20, 21, 22, 23, 24, 25, 26]). While solutions with specifically designed architectures are guaranteed to be compliant to the physical constraints, creating such architectures demands extensive domain knowledge and may not be easily adaptable to other problems. Additionally, the expressivity and training complexity could be limited in these cases. Soft constraints are implemented by incorporating physics-informed terms into the loss function. For example, [27, 28, 29, 30, 31, 32, 33, 12, 8]. While more flexible in terms of neural network architecture design, this approach still requires precise knowledge of physics in the form of differential equations, variational problems, etc., which are not always available, especially when the system is not fully understood by humans.

In-context operator learning excels at addressing a broad spectrum of physical problems using a single neural network. The limited flexibility and generalizability of the previously mentioned approaches hinder their application to in-context operator learning. This limitation motivates our exploration in this paper, where we introduce a new method to incorporate physical knowledge: through “captions”.

## 2.3 Multi-Modal Models

Unimodal language models solely rely on text data for training, limiting their ability to comprehend the visual world. In contrast, multimodal language models are trained on data in multiple forms, including texts and images, enabling them to understand the visual world. We refer readers to the survey [34] on this topic.

To fuse different modal data, one approach involves combining the extracted features or embeddings from different modal data and then feeding these embeddings into the same model [35, 36, 37, 38, 39, 40, 41, 42, 43, 44, 45]. Another approach converts other modal data into language data and uses these language representations as inputs for language models [46]. Some studies combine both

techniques, utilizing both extracted features and converted language data as inputs to language models [47, 48].

During the training phase, due to the constraints of computational complexity, many models (such as [43, 44, 36]) freeze the parameters of the language models and only train the parameters of the other components, like data embeddings or bridging projections. The performance of this training strategy is compared to end-to-end fine-tuning in [35].

In this paper, we integrate embeddings of function data and language captions into the same model, instead of converting one form of data into another, and fine-tune the model in an end-to-end way.

### 3 Dataset and GPT-Assisted Caption Generation

In this study, we inherit the function data from [1]. This dataset contains 19 types of operator learning problems, including forward and inverse ordinary differential equations (ODEs), partial differential equations (PDEs) and mean-field control problems, each spanning a continuous range of operators. Within the training dataset, each type of problem comes with 1,000 distinct operators. For every operator, there are 100 condition-QoI pairs governed by such a shared operator. During training, one can randomly sample from these 100 pairs as “examples” and “questions” to build an instance of prompt and label. In the testing dataset, each type of problem is represented by an additional 100 unique operators. Every operator is associated with 5 sets of condition-QoI pairs, and each set has 6 such pairs. For testing purposes, the initial  $J$  pairs in each set can serve as “examples”, while the final pair acts as the “question” for  $J$ -shot learning, with  $J$  ranging from zero to five. This means the testing dataset consists of  $19 \times 500$  sets, translating to  $19 \times 500$  learning cases for every value of  $J$ .

For multi-modal learning, we produced 160 captions per operator for training and an additional 40 for testing. These captions are of two categories: vague and precise, depending on whether they reveal the actual parameter values that determine the operator, for example, the decay rate of a damped oscillator, the boundary condition of PDEs, or the terminal cost in a mean-field control problem. We refer the reader to [1] for more details on parameters.

Here’s how we generated these captions.

First, we utilized the GPT-4 API to create two categories of captions for every problem type. To reduce the workload, we merged the forward and inverse problems for ODEs/PDEs when generating captions, and then manually specified the condition and QoI terms to distinguish between the two. Similarly, for the mean-field control problems we merged the problems with condition/QoI terms in different time intervals. From both the vague and precise categories, we generated 100 captions each, allocating 80 for training and 20 for testing. Most of the AI-produced captions were suitable, while a few necessitated slight

manual adjustments.

For the vague group, we instructed GPT-4 to use natural language to describe the equation or tell the form of the equation without revealing the specific parameter values. For the precise group, we instructed GPT-4 to leave placeholders for the actual parameters.

During training, for each prompt instance, a caption is randomly selected from all the training captions, including vague ones and precise ones, associated with the operator. If a precise caption is selected, the placeholders for parameters are replaced with the actual parameter values. It’s worth noting that for mean-field control problems, since the parameters are functional, we adopted a discretization approach to represent them effectively. Similarly, a caption is randomly selected from the testing group for each prompt instance during testing.

To provide a clearer understanding of the captions used, we present some examples in the Appendix.

## 4 The ICON-LM Model

### 4.1 Overview

The ICON-LM model aims to take as input the caption as well as multiple pairs of conditions and QoIs, each condition or QoI being a function represented by a set of key-value pairs.

The original ICON architecture in [1] consists of two transformers: an encoder and a decoder. Also, for every prompt instance, the model is solely trained to perform in-context operator learning with a certain number of examples. Its capability to adapt to varying numbers of examples comes from the inclusion of different numbers of examples in distinct instances within the batch.

We identified this architecture and training method as inefficient. In this paper, we propose to merge the encoder and decoder into a single transformer, so that we can train a language-model-like architecture, or directly fine-tune existing language models, for in-context operator learning. Moreover, we train the model to execute in-context operator learning in an autoregressive manner, i.e., the model predicts the QoI in each example based on preceding examples, similar to the “next-token prediction” training scheme in language models. This training scheme is more efficient, as for each prompt instance, the model simultaneously performs in-context operator learning with varying numbers of examples, ranging from zero (with a caption) or one (without a caption) up to the maximum capacity.

While drawing parallels between language models and operator learning, it’s essential to underscore the distinctions and unique requirements of operator learning.

1. The model should be invariant to the permutation of key-value pairs within a function, since these key-value pairs are unordered.

2. The prediction of a QoI function should not be limited to a preset collection of function inputs but is applicable to any inputs, namely “queries” in [1].
3. For a QoI function, the outputs corresponding to specific queries should not be generated sequentially as in language models. Rather, these predictions should be made in parallel and independent of each other.

To address these requirements, we need to design customized input and output sequences, as well as a transformer mask, which will be discussed in the following subsections.

## 4.2 Input Tokens

The input sequence consists of the caption tokens and function tokens constructed from the key-value pairs. In [1] each key-value pair is converted into a token by concatenating the key, value, as well as a one-hot index vector which distinguishes different functions. Here, we recognize that the one-hot index vector is equivalent to adding the positional encoding after the linear embedding layer. We thus delete the index vector and only use the key and value in function tokens for simplicity.

The model predicts the QoI function based on the preceding examples. Crucially, these predictions should be made for any function inputs, in parallel and independent of each other. To address such requirements, in addition to the condition function tokens and QoI function tokens, we also include the “query tokens” in the sequence, which are the vectors representing the keys of the QoI function. Unlike the approach in [46], where queries are created solely for the last example, in our method, queries are created for each example. It’s important to note that within this framework, the term “queries” differs from those tied to the transformer model’s attention mechanism.

In table 1, we show the tokens of the  $j$ -th example for the one-dimensional forward ODE problem, where the condition consists of the control  $c: [0, T] \rightarrow \mathbb{R}$  and the initial condition  $u(0)$ ; the QoI is the state  $u: [0, T] \rightarrow \mathbb{R}$ .

		condition	QoI	query
key	term	$\begin{pmatrix} 0 & 0 & \dots & 0 & 1 \end{pmatrix}$	$\begin{pmatrix} 0 & 0 & \dots & 0 \end{pmatrix}$	$\begin{pmatrix} 0 & 0 & \dots & 0 \end{pmatrix}$
	time	$\begin{pmatrix} t_1 & t_2 & \dots & t_{n_j-1} & 0 \end{pmatrix}$	$\begin{pmatrix} \tau_1 & \tau_2 & \dots & \tau_{m_j} \end{pmatrix}$	$\begin{pmatrix} \tau_1 & \tau_2 & \dots & \tau_{m_j} \end{pmatrix}$
	space	$\begin{pmatrix} 0 & 0 & \dots & 0 & 0 \end{pmatrix}$	$\begin{pmatrix} 0 & 0 & \dots & 0 \end{pmatrix}$	$\begin{pmatrix} 0 & 0 & \dots & 0 \end{pmatrix}$
	value	$\begin{pmatrix} c(t_1) & c(t_2) & \dots & c(t_{n_j-1}) & u(0) \end{pmatrix}$	$\begin{pmatrix} u(\tau_1) & u(\tau_2) & \dots & u(\tau_{m_j}) \end{pmatrix}$	$\begin{pmatrix} 0 & 0 & \dots & 0 \end{pmatrix}$

Table 1: The tokens for the  $j$ -th example for the one-dimensional forward ODE problem. Each column represents a token. We use  $n_j - 1$  key-value pairs to represent  $c$ , one key-value pair for  $u(0)$ , and  $m_j$  key-value pairs for  $u$ . Note that in the first row, we use the indicators 0 and 1 to distinguish different terms in the condition, i.e.,  $c$  and  $u(0)$ . The third row is populated with zeros since there are no spatial coordinates in this problem. The keys in query tokens are the same as those for QoIs, but the values are populated with zero.



### 4.3 Model and Transformer Mask

Every condition, QoI, and query token is transformed into an embedding vector via a shared embedding layer (e.g., a linear layer or a shallow multi-layer perceptron). These embedding vectors are then concatenated and appended to the caption embeddings, which are transformed from caption tokens with a different embedding layer.

Before being supplied to the transformer, the input sequence is added with positional encoding. For caption embeddings, the positional encoding mirrors that utilized in language models. To distinguish different examples and different types of tokens (whether condition, QoI, or query) within each example, we also introduce learnable positional encoding for the function embeddings. Notably, to ensure the model remains invariant to the order of key-value pairs within a function, every token of the same type within an example shares the same positional encoding. As an illustration, for five distinct condition-QoI examples, there would be a total of 15 learnable vectors designated for positional encoding: five each for condition tokens, QoI tokens, and query tokens.

After being added with positional encoding, the input sequence is supplied to a transformer. The output sequence of the transformer is then fed into a head layer (e.g., a linear layer or a shallow multi-layer perceptron), to align the dimensions with those of the QoI values. Note that in the output sequence, we only keep the ones corresponding to the query tokens, since these are the ones that aim to predict the QoI values corresponding to the queries. The input/output sequence and the model architecture are depicted in Figure 2a.

The design of the transformer mask is the key challenge in the ICON-LM model due to the following constraints.

1. The model predicts the QoI value, taking into account (1) all the caption tokens, (2) all the conditions and QoI tokens from preceding examples, (3) all the condition tokens of the current example, as well as (4) the current query token.
2. When making the prediction, it's crucial to prevent inadvertent leakage of the QoI tokens in the current example, since the values in the QoI tokens are the target of the prediction.
3. Also, the queries should not attend to each other, as the predictions should be independent.
4. The invariance to the permutation of key-value pairs within a function should be maintained.
5. In the end, the mask, denoted by  $M$ , should satisfy  $MM = M$ , which ensures that there is no unintentional information leakage due to indirect attention, e.g., the token  $c$ 's information is leaked to the token  $a$  through  $a$  attending to  $b$ , and  $b$  attending to  $c$ .

We carefully designed the mask that satisfies all the constraints above, illustrated in Figure 2b. The mask block for caption tokens is lower triangular,

in consistency with the existing generative language model. The other blocks are not lower triangular for the sake of permutation invariance. The blocks for queries are diagonal, indicating that the query tokens do not attend to each other.

Due to various lengths of captions and key-value pairs within a function, we may have to include placeholder tokens in the input sequence to maintain a consistent length in a batch. These placeholder tokens need to be ignored in the attention mechanism. We accomplish this by carrying out an element-wise multiplication of the previously constructed mask with another mask specifically designed to indicate these placeholder tokens, in which the columns corresponding to the placeholder tokens are set to zero, and the rest are set to one.

Since the model architecture is similar to that of language models, we can directly fine-tune existing language models for in-context operator learning, especially for multi-modal learning. The only changes are the embedding layer for function tokens and the head layer, as well as the customized transformer mask.

#### 4.4 Training and Inference

We can train the ICON-LM model to execute in-context operator learning, with the option of including or excluding captions. The loss function is the mean squared error between the predicted QoI values and the actual labels. For training inclusive of captions, the loss function is calculated from the first example prediction up to the last, with the first example prediction being a zero-shot – a prediction solely based on the caption and condition, excluding any other examples. When training without captions, we exclude the caption from the input sequence and calculate the loss function from the second example’s predictions to the last, bypassing zero-shot learning as it is not meaningful to predict the QoI value without any example or caption. The total loss for multi-modal training comprises the losses from both options.

During the inference stage, the new question condition and query tokens are considered “the last example” and appended to the input sequence. The QoI tokens for the new question are not required.

Note that some components of the input sequence can, or should, be excluded in certain scenarios. This affects the corresponding rows and columns of the masks as well. In this paper, we applied the following four variations:

1. **Training with caption:** Here, predictions are needed for all queries. While the full mask described in section 4.3 is applicable, we find that the QoI tokens in the last example are never attended by other tokens. Hence, they are omitted from the input sequence to minimize the computational load.
2. **Training without caption:** In this scenario, predictions are required for all queries, except those in the first example. We exclude the caption tokens, the query tokens in the first example, and the QoI tokens in the last example from the input sequence.

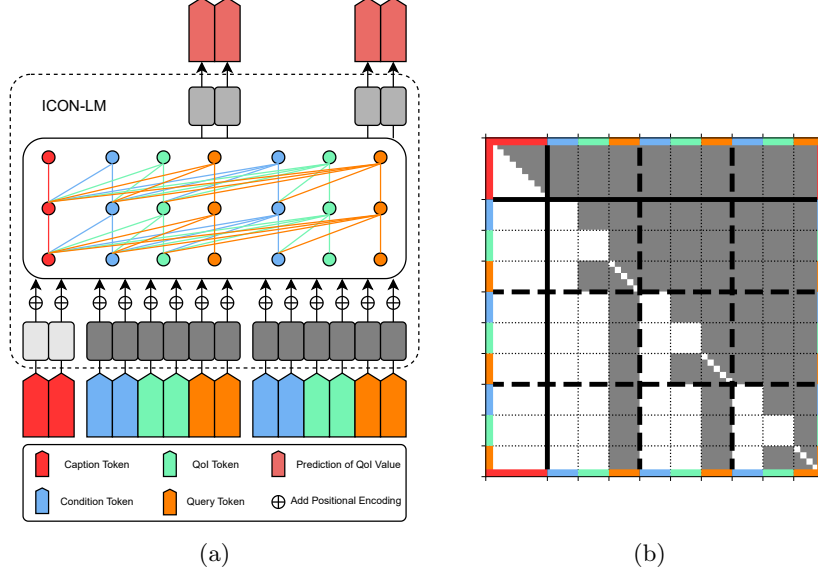


Figure 2: (a) Depiction of the input/output sequence and model architecture of ICON-LM. For clarity, we present only two examples. The model of ICON-LM is highlighted by the black dashed enclosure. Grey rectangles with varying grey scales represent the input embedding layer and output head layer. The connections between different component blocks in the transformer are a simplified illustration of the customized attention mechanism. (b) The transformer mask for ICON-LM, with white cells representing ones, and grey cells representing zeros. As illustrated, the mask for three examples can be divided into  $10 \times 10$  blocks. Black solid lines separate blocks for captions and examples, while black dashed lines separate examples. Along the boundary, varying colors indicate different components: red for captions, blue for conditions, green for QoIs, and orange for queries, consistent with (a).

3. **Inference with caption:** Here, the focus lies only on the prediction for “the last example”. As such, the query tokens from all preceding examples can be omitted from the input sequence, along with the last example’s QoI tokens, which are absent during the inference stage.
4. **Inference without caption:** This case parallels the previous “inference with caption” scenario, except for the omission of the caption tokens from the input sequence.

These four mask variations are depicted in Figure 3.

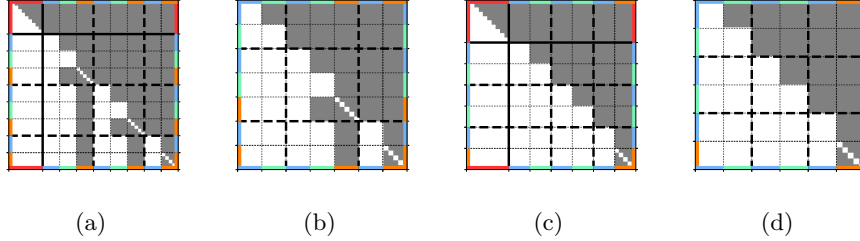


Figure 3: Four transformer mask variants for ICON-LM. (a) Training with caption. (b) Training without caption. (c) Inference with caption. (d) Inference without caption. Varying colors along the boundary indicate different components, which are consistent with Figure 2b.

## 5 Experiments

### 5.1 Single-Modal In-Context Operator Learning

This section serves to show the performance of ICON-LM for single-modal in-context operator learning, i.e., without captions, and compare it with the baseline, the encoder-decoder ICON model introduced in [1].

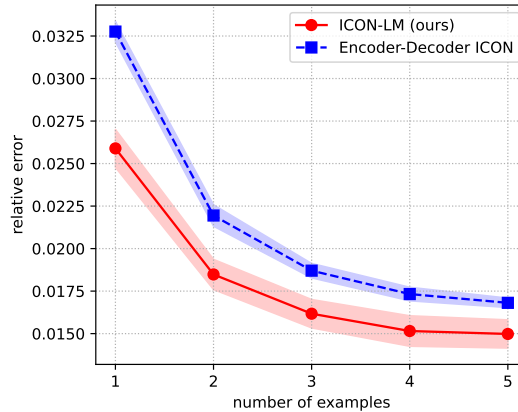


Figure 4: Comparison of ICON-LM (ours) and encoder-decoder ICON for single-modal in-context operator learning. We calculate the relative testing error averaged over all 19 types of problems, and take the mean and standard deviation over three runs, shown as the solid line and the shaded area, respectively.

The training and testing datasets are inherited from [1]. We also adopt the same training configurations for the encoder-decoder ICON, as well as the testing setups for both models. Specifically, the encoder-decoder ICON is trained with  $J$  examples alongside one question, with  $J$  randomly selected between one

and five for each prompt instance. In contrast, ICON-LM is trained with six examples per instance, allowing for concurrent one-shot to five-shot learning. We emphasize that although the number of examples varies between the two models, the total training data remains consistent for both. In both setups, the examples and the question in every prompt instance are drawn randomly from a set of 100 condition-QoI pairs governed by the same operator in the training dataset.

The encoder-decoder ICON encompasses approximately 31.6 million parameters, whereas the ICON-LM operates with nearly half that number, at around 15.8 million. This substantial reduction is credited to the ICON-LM’s simplified architecture, which employs a single transformer roughly equivalent in size to either the encoder or decoder in the encoder-decoder ICON. Both models are trained for 1 million steps, with the same setups for optimizer and learning rate schedule. We put details in the appendix.

The batch size is 32 for encoder-decoder ICON, and 24 for ICON-LM. Compared with encoder-decoder ICON, the larger sequence length (about  $\times 1.5$ ) in ICON-LM requires more GPU memory, but this is largely offset by the single transformer design, and slightly smaller batch size. With such setups, both models take about 19GB GPU memory, and can fit in one NVIDIA GeForce RTX 4090 GPU with 24 GB memory. As for the time consumption, the training takes about 41.5 hours for the encoder-decoder ICON, and about 37.5 hours for ICON-LM.

We compare the relative testing error averaged over all 19 types of problems for cases from one-shot to five-shot learning. The results are shown in Figure 4. It’s clear that ICON-LM outperforms encoder-decoder ICON in all cases.

## 5.2 Multi-Modal In-Context Operator Learning

In this section, we demonstrate the effectiveness of multi-modal in-context operator learning. We fine-tuned the tiny GPT-2 model with full parameters in the ICON-LM framework. The training setup is the same as ICON-LM in Section 5.1, except that the total loss for multi-modal training comprises the losses with captions and without captions, and the batch size is 10. The training takes about 5.5 days on dual NVIDIA GeForce RTX 4090 GPUs.

In Figure 5, we present a comparison of the average relative testing error across all 19 problem types, examining the performance when learning without captions, with vague captions, and with precise captions. A comprehensive comparison for each specific problem type, along with an analysis of error distribution across training and testing datasets for generalization analysis, can be found in the Appendix.

It’s clear that the testing error decreases as we move from no caption to vague caption to precise caption, especially for zero-shot. This shows the effectiveness of the caption in helping the model to learn the operator.

It is worth noting that zero-shot learning with vague captions performs surprisingly well for some problems. These include the forward and inverse damped

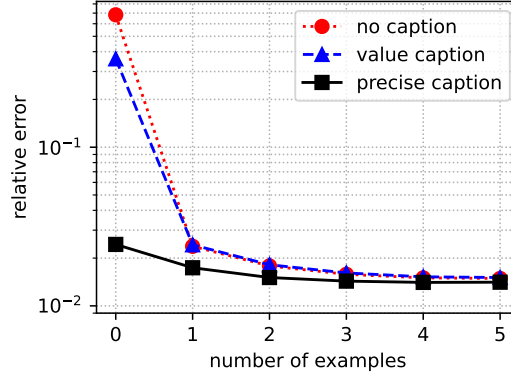


Figure 5: Comparison of ICON-LM with vague captions, precise captions, and no captions for multi-modal in-context operator learning.

oscillator series problems, the inverse Poisson equation problem, and the mean-field control problem with  $g$  parameters, mapping from 2D density field to 2D density field. These results are not as surprising upon closer examination, since the operator parameters for these problems can be inferred from the conditions provided, once the problem type is identified with the vague captions. For instance, the decay rate of the damped oscillator can be computed from a segment of the time series, the boundary conditions of the Poisson equation are encapsulated within the conditions of  $u(x)$ , and the terminal cost in the mean-field control problem can be derived from the density field during the interval  $t \in [0, 0.5]$ . These examples highlight the impressive capabilities of the ICON-LM framework in combining multi-modal information to learn the operator.

### 5.3 Numerical Task Helps the Language Model Understand Captions

The inclusion of captions has been shown to enhance a model’s ability to learn operations. In this section, we demonstrate that multi-modal in-context learning not only aids in operator learning but also improves the language model’s comprehension of captions, even without direct fine-tuning for caption generation or classification. To investigate this, we compare the sentence embeddings of captions generated by the standard GPT-2 model with those from the multi-modal fine-tuned GPT-2 variant used in Section 5.2. The embeddings are calculated by averaging the last layer’s hidden states.

Given that some types of problems are merged when generating captions with GPT-4 API, as outlined in Section 3, we have nine categories of captions here, 200 in each category. Our goal is to assess the degree to which these embeddings form separable clusters. To this end, we employ the Silhouette score [49], a metric widely utilized for evaluating clustering performance. The

results, presented in Table 2, include scores for full embeddings as well as for those reduced in dimensionality through methods such as t-SNE [50], PCA [51], and Isomap [52]. After fine-tuning, the observed increase in the Silhouette score across all dimensionality reduction methods suggests that engaging in numerical prediction tasks enables the language model to attain a better understanding of the captions. We also visualize the embedding clusters in Figure 6 with t-SNE, where one can clearly see that the categories are more separable after fine-tuning.

	Standard GPT-2	Finetuned GPT-2
Full Embedding	-0.139	<b>-0.0124</b>
t-SNE 2D	-0.161	<b>-0.0430</b>
PCA 100D	-0.139	<b>-0.0127</b>
PCA 10D	-0.143	<b>-0.0198</b>
Isomap 100D	-0.0694	<b>0.00361</b>
Isomap 10D	-0.0932	<b>0.00397</b>

Table 2: Silhouette scores for sentence embeddings of captions processed by the standard GPT-2 model and the multi-modal fine-tuned GPT-2 variant. Higher scores, highlighted in bold, indicate a more accurate fit of the inherent clusters and associated labels, i.e., better comprehension of the captions.

## 6 Summary

We present a novel approach to scientific machine learning with in-context operator learning, transforming it into a multi-modal framework by introducing “captions”. These captions incorporate human knowledge about the operator, in the form of natural language descriptions and equations. We also introduce a more efficient neural network architecture for multi-modal in-context operator learning called “ICON-LM”. This architecture closely aligns with language models, with the exception of novel input sequences and transformer mask designs.

In the experiments, we compared the ICON-LM model with the original encoder-decoder ICON model, in the single-modal learning scenario. The proposed ICON-LM model, comprising approximately half parameters, surpasses the performance of the encoder-decoder ICON model with less training time. This can be attributed that the encoder-decoder ICON model is trained with a fixed number of examples in each step, while the ICON-LM model is trained with varying numbers of examples concurrently in each training step.

We also fine-tuned GPT-2 model for multi-modal in-context operator learning. We found that captions’ presence, especially precise ones that disclose the parameters in the operators, significantly improved learning performance when the number of examples was limited, showing impressive capabilities of the ICON-LM framework in combining multi-modal information to learn the

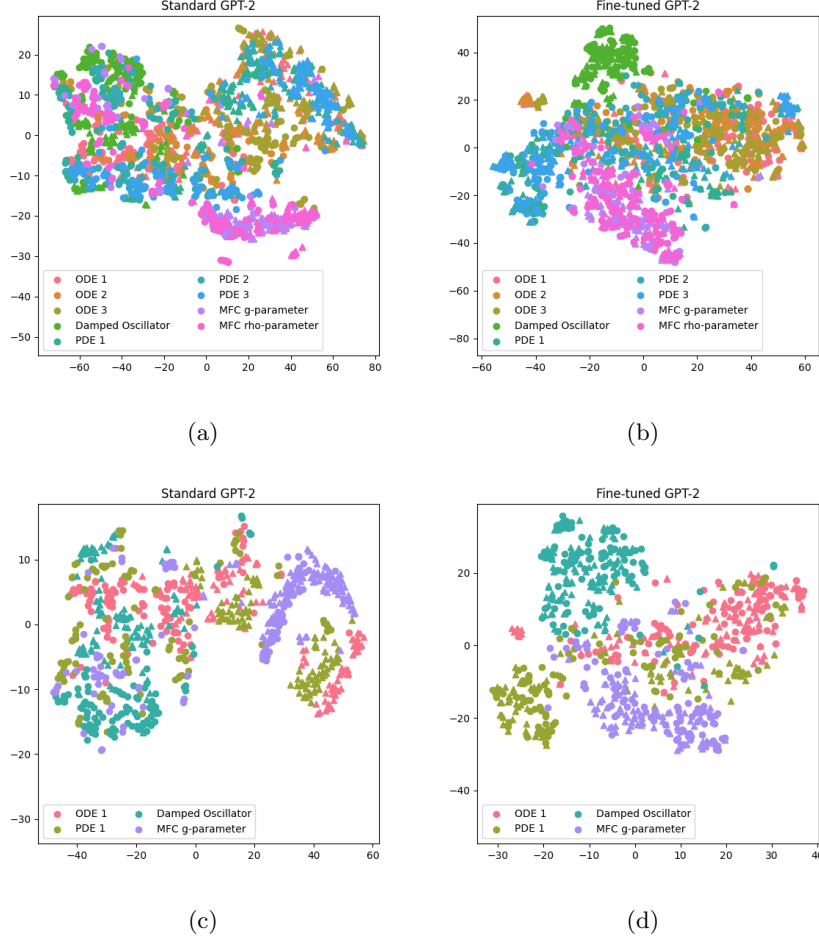


Figure 6: Visualization of caption embeddings reduced to 2D with t-SNE. (a) Standard GPT-2, all categories. (b) Fine-tuned GPT-2, all categories. (c) Standard GPT-2, selected categories. (d) Fine-tuned GPT-2, selected categories.

operator. Also, multi-modal fine-tuning enhanced the language model’s comprehension of captions, even without direct fine-tuning for caption generation or classification. This suggests that the ICON-LM framework can be used to improve the language model’s understanding of mathematical equations and scientific concepts, which could be beneficial for other applications.

In this paper, the usage of “caption” is limited to the model input. In the future, we wish to explore the generation of captions with in-context operator learning. Specifically, we’re interested in producing operator descriptions as equations, in natural language, or a blend of both, based on examples from



sensory data. Such advancements could pave the way for automated scientific modeling and data analysis within the framework of in-context learning.

## Acknowledgement

This work is partially funded by AFOSR MURI FA9550-18-502, and ONR MURI N00014-20-1-2787. We would like to express our gratitude to ChatGPT for enhancing the wording during the paper writing phase. We also want to thank Dr. Tingwei Meng and Dr. Hedi Xia for the helpful discussions.

## References

- [1] Liu Yang, Siting Liu, Tingwei Meng, and Stanley J Osher. In-context operator learning with data prompts for differential equation problems. *Proceedings of the National Academy of Sciences*, 120(39):e2310142120, 2023.
- [2] Tianping Chen and Hong Chen. Universal approximation to nonlinear operators by neural networks with arbitrary activation functions and its application to dynamical systems. *IEEE transactions on neural networks*, 6(4):911–917, 1995.
- [3] Tianping Chen and Hong Chen. Approximation capability to functions of several variables, nonlinear functionals, and operators by radial basis function neural networks. *IEEE Transactions on Neural Networks*, 6(4):904–910, 1995.
- [4] Yuehaw Khoo, Jianfeng Lu, and Lexing Ying. Solving parametric PDE problems with artificial neural networks. *European Journal of Applied Mathematics*, 32(3):421–435, 2021.
- [5] Yinhao Zhu and Nicholas Zabaras. Bayesian deep convolutional encoder-decoder networks for surrogate modeling and uncertainty quantification. *Journal of Computational Physics*, 366:415–447, 2018.
- [6] Zichao Long, Yiping Lu, Xianzhong Ma, and Bin Dong. PDE-Net: Learning PDEs from data. In *International conference on machine learning*, pages 3208–3216. PMLR, 2018.
- [7] Lu Lu, Pengzhan Jin, Guofei Pang, Zhongqiang Zhang, and George Em Karniadakis. Learning nonlinear operators via deepnet based on the universal approximation theorem of operators. *Nature machine intelligence*, 3(3):218–229, 2021.
- [8] Sifan Wang, Hanwen Wang, and Paris Perdikaris. Learning the solution operator of parametric partial differential equations with physics-informed DeepOnets. *Science advances*, 7(40):eabi8605, 2021.

- [9] Zongyi Li, Nikola Borislavov Kovachki, Kamyar Azizzadenesheli, Burigede liu, Kaushik Bhattacharya, Andrew Stuart, and Anima Anandkumar. Fourier neural operator for parametric partial differential equations. In *International Conference on Learning Representations*, 2021.
- [10] Nikola Kovachki, Zongyi Li, Burigede Liu, Kamyar Azizzadenesheli, Kaushik Bhattacharya, Andrew Stuart, and Anima Anandkumar. Neural operator: Learning maps between function spaces with applications to PDEs. *Journal of Machine Learning Research*, 24(89):1–97, 2023.
- [11] Kaushik Bhattacharya, Bamdad Hosseini, Nikola B Kovachki, and Andrew M Stuart. Model reduction and neural networks for parametric PDEs. *The SMAI journal of computational mathematics*, 7:121–157, 2021.
- [12] Zongyi Li, Hongkai Zheng, Nikola Kovachki, David Jin, Haoxuan Chen, Burigede Liu, Kamyar Azizzadenesheli, and Anima Anandkumar. Physics-informed neural operator for learning partial differential equations. *arXiv preprint arXiv:2111.03794*, 2021.
- [13] Rishi Bommasani, Drew A Hudson, Ehsan Adeli, Russ Altman, Simran Arora, Sydney von Arx, Michael S Bernstein, Jeannette Bohg, Antoine Bosselut, Emma Brunskill, et al. On the opportunities and risks of foundation models. *arXiv preprint arXiv:2108.07258*, 2021.
- [14] Dmitrii Kochkov, Jamie A Smith, Ayya Alieva, Qing Wang, Michael P Brenner, and Stephan Hoyer. Machine learning-accelerated computational fluid dynamics. *Proceedings of the National Academy of Sciences*, 118(21):e2101784118, 2021.
- [15] Georgios Kissas, Jacob H Seidman, Leonardo Ferreira Guilhoto, Victor M Preciado, George J Pappas, and Paris Perdikaris. Learning operators with coupled attention. *Journal of Machine Learning Research*, 23(215):1–63, 2022.
- [16] Somdatta Goswami, Katiana Kontolati, Michael D Shields, and George Em Karniadakis. Deep transfer operator learning for partial differential equations under conditional shift. *Nature Machine Intelligence*, pages 1–10, 2022.
- [17] Min Zhu, Handi Zhang, Anran Jiao, George Em Karniadakis, and Lu Lu. Reliable extrapolation of deep neural operators informed by physics or sparse observations. *Computer Methods in Applied Mechanics and Engineering*, 412:116064, 2023.
- [18] Adam Subel, Yifei Guan, Ashesh Chattopadhyay, and Pedram Hassanzadeh. Explaining the physics of transfer learning in data-driven turbulence modeling. *PNAS nexus*, 2(3):pgad015, 2023.

- [19] George Em Karniadakis, Ioannis G Kevrekidis, Lu Lu, Paris Perdikaris, Sifan Wang, and Liu Yang. Physics-informed machine learning. *Nature Reviews Physics*, 3(6):422–440, 2021.
- [20] Linfeng Zhang, Jiequn Han, Han Wang, Roberto Car, and EJPRL Weinan. Deep potential molecular dynamics: a scalable model with the accuracy of quantum mechanics. *Physical review letters*, 120(14):143001, 2018.
- [21] David Pfau, James S Spencer, Alexander GDG Matthews, and W Matthew C Foulkes. Ab initio solution of the many-electron schrödinger equation with deep neural networks. *Physical Review Research*, 2(3):033429, 2020.
- [22] GP Purja Pun, R Batra, R Ramprasad, and Y Mishin. Physically informed artificial neural networks for atomistic modeling of materials. *Nature communications*, 10(1):2339, 2019.
- [23] Julia Ling, Andrew Kurzawski, and Jeremy Templeton. Reynolds averaged turbulence modelling using deep neural networks with embedded invariance. *Journal of Fluid Mechanics*, 807:155–166, 2016.
- [24] Pengzhan Jin, Zhen Zhang, Aiqing Zhu, Yifa Tang, and George Em Karniadakis. SympNets: Intrinsic structure-preserving symplectic networks for identifying Hamiltonian systems. *Neural Networks*, 132:166–179, 2020.
- [25] Bethany Lusch, J Nathan Kutz, and Steven L Brunton. Deep learning for universal linear embeddings of nonlinear dynamics. *Nature communications*, 9(1):4950, 2018.
- [26] Marios Mattheakis, Pavlos Protopapas, David Sondak, Marco Di Giovanni, and Efthimios Kaxiras. Physical symmetries embedded in neural networks. *arXiv preprint arXiv:1904.08991*, 2019.
- [27] Weinan E, Jiequn Han, and Arnulf Jentzen. Deep learning-based numerical methods for high-dimensional parabolic partial differential equations and backward stochastic differential equations. *Communications in mathematics and statistics*, 5(4):349–380, 2017.
- [28] Jiequn Han, Arnulf Jentzen, and Weinan E. Solving high-dimensional partial differential equations using deep learning. *Proc. Natl. Acad. Sci. USA*, 115(34):8505–8510, 2018.
- [29] Justin Sirignano and Konstantinos Spiliopoulos. DGM: a deep learning algorithm for solving partial differential equations. *J. Comput. Phys.*, 375:1339–1364, 2018.
- [30] Weinan E and Bing Yu. The deep Ritz method: a deep learning-based numerical algorithm for solving variational problems. *Commun. Math. Stat.*, 6(1):1–12, 2018.

- [31] M. Raissi, P. Perdikaris, and G. E. Karniadakis. Physics-informed neural networks: a deep learning framework for solving forward and inverse problems involving nonlinear partial differential equations. *J. Comput. Phys.*, 378:686–707, 2019.
- [32] Yaohua Zang, Gang Bao, Xiaojing Ye, and Haomin Zhou. Weak adversarial networks for high-dimensional partial differential equations. *J. Comput. Phys.*, 411:109409, 14, 2020.
- [33] Lars Ruthotto, Stanley J. Osher, Wuchen Li, Levon Nurbekyan, and Samy Wu Fung. A machine learning framework for solving high-dimensional mean field game and mean field control problems. *Proc. Natl. Acad. Sci. USA*, 117(17):9183–9193, 2020.
- [34] Shukang Yin, Chaoyou Fu, Sirui Zhao, Ke Li, Xing Sun, Tong Xu, and Enhong Chen. A survey on multimodal large language models. *arXiv preprint arXiv:2306.13549*, 2023.
- [35] Danny Driess, Fei Xia, Mehdi SM Sajjadi, Corey Lynch, Aakanksha Chowdhery, Brian Ichter, Ayzaan Wahid, Jonathan Tompson, Quan Vuong, Tianhe Yu, et al. PaLM-E: An embodied multimodal language model. *arXiv:2303.03378*, 2023.
- [36] Jean-Baptiste Alayrac, Jeff Donahue, Pauline Luc, Antoine Miech, Iain Barr, Yana Hasson, Karel Lenc, Arthur Mensch, Katherine Millican, Malcolm Reynolds, et al. Flamingo: a visual language model for few-shot learning. *Advances in Neural Information Processing Systems*, 35:23716–23736, 2022.
- [37] Junnan Li, Dongxu Li, Silvio Savarese, and Steven Hoi. BLIP-2: Bootstrapping language-image pre-training with frozen image encoders and large language models. *arXiv preprint arXiv:2301.12597*, 2023.
- [38] Xiaoman Zhang, Chaoyi Wu, Ziheng Zhao, Weixiong Lin, Ya Zhang, Yanfeng Wang, and Weidi Xie. PMC-VQA: Visual instruction tuning for medical visual question answering. *arXiv preprint arXiv:2305.10415*, 2023.
- [39] Haotian Liu, Chunyuan Li, Qingyang Wu, and Yong Jae Lee. Visual instruction tuning. *arXiv:2304.08485*, 2023.
- [40] Renrui Zhang, Jiaming Han, Aojun Zhou, Xiangfei Hu, Shilin Yan, Pan Lu, Hongsheng Li, Peng Gao, and Yu Qiao. LLaMA-adapter: Efficient fine-tuning of language models with zero-init attention. *arXiv preprint arXiv:2303.16199*, 2023.
- [41] Renjie Pi, Jiahui Gao, Shizhe Diao, Rui Pan, Hanze Dong, Jipeng Zhang, Lewei Yao, Jianhua Han, Hang Xu, and Lingpeng Kong Tong Zhang. DetGPT: Detect what you need via reasoning. *arXiv preprint arXiv:2305.14167*, 2023.

- [42] Hang Zhang, Xin Li, and Lidong Bing. Video-LLaMA: An instruction-tuned audio-visual language model for video understanding. *arXiv preprint arXiv:2306.02858*, 2023.
- [43] Maria Tsimpoukelli, Jacob L Menick, Serkan Cabi, SM Eslami, Oriol Vinyals, and Felix Hill. Multimodal few-shot learning with frozen language models. *Advances in Neural Information Processing Systems*, 34:200–212, 2021.
- [44] Deyao Zhu, Jun Chen, Xiaoqian Shen, Xiang Li, and Mohamed Elhoseiny. MiniGPT-4: Enhancing vision-language understanding with advanced large language models. *arXiv preprint arXiv:2304.10592*, 2023.
- [45] Anthony Brohan, Noah Brown, Justice Carbajal, Yevgen Chebotar, Xi Chen, Krzysztof Choromanski, Tianli Ding, Danny Driess, Avinava Dubey, Chelsea Finn, Pete Florence, Chuyuan Fu, Montse Gonzalez Arenas, Keerthana Gopalakrishnan, Kehang Han, Karol Hausman, Alex Herzog, Jasmine Hsu, Brian Ichter, Alex Irpan, Nikhil Joshi, Ryan Julian, Dmitry Kalashnikov, Yuheng Kuang, Isabel Leal, Lisa Lee, Tsang-Wei Edward Lee, Sergey Levine, Yao Lu, Henryk Michalewski, Igor Mordatch, Karl Pertsch, Kanishka Rao, Krista Reymann, Michael Ryoo, Grecia Salazar, Pannag Sanketi, Pierre Sermanet, Jaspier Singh, Anikait Singh, Radu Soricut, Huong Tran, Vincent Vanhoucke, Quan Vuong, Ayzaan Wahid, Stefan Welker, Paul Wohlhart, Jialin Wu, Fei Xia, Ted Xiao, Peng Xu, Sichun Xu, Tianhe Yu, and Brianna Zitkovich. RT-2: Vision-language-action models transfer web knowledge to robotic control. 2023.
- [46] Zhengyuan Yang, Zhe Gan, Jianfeng Wang, Xiaowei Hu, Yumao Lu, Zicheng Liu, and Lijuan Wang. An empirical study of GPT-3 for few-shot knowledge-based VQA. In *Proceedings of the AAAI Conference on Artificial Intelligence*, volume 36, pages 3081–3089, 2022.
- [47] KunChang Li, Yinan He, Yi Wang, Yizhuo Li, Wenhai Wang, Ping Luo, Yali Wang, Limin Wang, and Yu Qiao. VideoChat: Chat-centric video understanding. *arXiv preprint arXiv:2305.06355*, 2023.
- [48] Peng Gao, Jiaming Han, Renrui Zhang, Ziyi Lin, Shijie Geng, Aoju Zhou, Wei Zhang, Pan Lu, Conghui He, Xiangyu Yue, et al. LLaMA-adapter V2: Parameter-efficient visual instruction model. *arXiv preprint arXiv:2304.15010*, 2023.
- [49] Peter J Rousseeuw. Silhouettes: a graphical aid to the interpretation and validation of cluster analysis. *Journal of computational and applied mathematics*, 20:53–65, 1987.
- [50] Laurens Van der Maaten and Geoffrey Hinton. Visualizing data using t-sne. *Journal of machine learning research*, 9(11), 2008.

- [51] Svante Wold, Kim Esbensen, and Paul Geladi. Principal component analysis. *Chemometrics and intelligent laboratory systems*, 2(1-3):37–52, 1987.
- [52] Mukund Balasubramanian and Eric L Schwartz. The isomap algorithm and topological stability. *Science*, 295(5552):7–7, 2002.

## Appendix

### Neural Network and Training Configurations

The transformer used in Section 5.1 is configured as in Table 3. Both the embedding layer and head layer are linear layers. For the fine-tuned GPT-2 model, we apply shallow multi-layer perceptrons as the embedding layer for function tokens as well as the head layer, with one hidden layer of dimension 1024. We utilize the AdamW optimizer with a warmup-cosine-decay schedule, employing the configuration in Table 4.

Table 3: Transformer Configuration

Layers	6
Heads in Multi-Head Attention	8
Input/Output Dimension of Each Layer	256
Dimension of Query/Key/Value in Attention Function	256
Hidden Dimension of Feedforward Networks	1024

Table 4: Configuration of Optimizer and Learning Rate Schedule

Initial Learning Rate	0.0
Peak Learning Rate	1e-4
End Learning Rate	0.0
Warmup Steps	First 10% of Total Steps
Cosine Annealing Steps	Remaining Steps
Global Norm Clip	1.0
Adam $\beta_1$	0.9
Adam $\beta_2$	0.999
Adam Weight Decay	1e-4

### Caption Examples

In this section, we show several examples of training and testing captions for three characteristic problem types: ODE 3 forward problem, PDE 3 forward problem, and MFC  $g$ -parameter  $1D \rightarrow 1D$ . For each type, we show four vague captions and four precise captions, with the first two used in training, and the last two for testing.

1. Caption examples for ODE 3 forward problem.

----Vague----

Variable  $u$ 's time derivative is  $\frac{du(t)}{dt} = a_1 \cdot u(t) + a_2 \cdot c(t) + a_3$ . Condition:  $u(0)$  and  $c(t)$ ,  $t \in [0,1]$ ,  $QoI$ :  $u(t)$ ,  $t \in [0,1]$ .

The ordinary differential equation represents the growth rate of variable  $u(t)$  in relation to itself and the control function  $c(t)$ . Condition:  $u(0)$  and  $c(t)$ ,  $t \in [0,1]$ , QoI:  $u(t)$ ,  $t \in [0,1]$ .

Derivation of  $u(t)$  in time following the formula  $\frac{du}{dt} = a_1 u(t) + a_2 c(t) + a_3$ . Condition:  $u(0)$  and  $c(t)$ ,  $t \in [0,1]$ , QoI:  $u(t)$ ,  $t \in [0,1]$ .

An ordinary differential equation with respect to time using a state variable  $u(t)$  and a control variable  $c(t)$ . Condition:  $u(0)$  and  $c(t)$ ,  $t \in [0,1]$ , QoI:  $u(t)$ ,  $t \in [0,1]$ .

----Precise----

Knowing that  $a_1 = -0.0124$ ,  $a_2 = 1.06$ ,  $a_3 = 0.105$ , the derivative  $\frac{du(t)}{dt} = -0.0124 \cdot u(t) + 1.06 \cdot c(t) + 0.105$ . Condition:  $u(0)$  and  $c(t)$ ,  $t \in [0,1]$ , QoI:  $u(t)$ ,  $t \in [0,1]$ .

The state variable changes according to  $\frac{du(t)}{dt} = 0.347 \cdot u(t) + 0.535 \cdot c(t) + 0.459$ . Condition:  $u(0)$  and  $c(t)$ ,  $t \in [0,1]$ , QoI:  $u(t)$ ,  $t \in [0,1]$ .

Express an ODE as  $\frac{du(t)}{dt} = -0.85 \cdot u(t) + 1.13 \cdot c(t) - 0.779$ . Condition:  $u(0)$  and  $c(t)$ ,  $t \in [0,1]$ , QoI:  $u(t)$ ,  $t \in [0,1]$ .

This differential equation  $\frac{du(t)}{dt} = 0.167 \cdot u(t) + 1.02 \cdot c(t) + 0.457$  shows how  $u(t)$  changes with time. Condition:  $u(0)$  and  $c(t)$ ,  $t \in [0,1]$ , QoI:  $u(t)$ ,  $t \in [0,1]$ .

## 2. Caption examples for PDE 3 forward problem.

----Vague----

The nonlinear PDE, written as  $-\lambda \frac{d^2 u}{dx^2} + a \cdot u^3 = c(x)$ , includes the variables  $u(x)$  and  $c(x)$ . Condition:  $c(x)$ ,  $x \in [0,1]$ , QoI:  $u(x)$ ,  $x \in [0,1]$ .

The nonlinear PDE,  $u''(x) - a \cdot u(x)^3 = c(x)$  roping in  $u(x)$  and  $c(x)$ . Condition:  $c(x)$ ,  $x \in [0,1]$ , QoI:  $u(x)$ ,  $x \in [0,1]$ .

Ponder upon this nonlinear PDE, involving the dependent variable  $u(x)$  and the term  $c(x)$  constituting the source. Condition:  $c(x)$ ,  $x \in [0,1]$ , QoI:  $u(x)$ ,  $x \in [0,1]$ .

This PDE,  $-\lambda \frac{d^2 u}{dx^2} + a \cdot u^3 = c(x)$ , involves the variables  $u(x)$  and  $c(x)$ . Condition:  $c(x)$ ,  $x \in [0,1]$ , QoI:  $u(x)$ ,  $x \in [0,1]$ .

----Precise----

For the given equation  $-\lambda \frac{d^2 u}{dx^2} + 1.16 \cdot u^3 = c(x)$ , we have the boundary conditions  $u(0) = -0.517$  and  $u(1) = -0.689$ . Condition:  $c(x)$ ,  $x \in [0,1]$ , QoI:  $u(x)$ ,  $x \in [0,1]$ .

The nonlinear PDE is  $-\lambda \frac{d^2 u}{dx^2} + 0.705 \cdot u^3 = c(x)$ , with  $u(0) = -0.319$  and  $u(1) = -0.667$ . Condition:  $c(x)$ ,  $x \in [0,1]$ , QoI:  $u(x)$ ,  $x \in [0,1]$ .



Equation  $-\frac{0.116}{2} \frac{d^2 u}{dx^2} + 0.586 \dot{u}^3 = c(x)$ , is our PDE with  $u(0) = 0.322$  and  $u(1) = -0.749$ . Condition:  $c(x)$ ,  $x \in [0,1]$ ,  $QoI: u(x)$ ,  $x \in [0,1]$ .  
Let's examine this PDE  $-\frac{0.139}{2} \frac{d^2 u}{dx^2} + 1.25 \dot{u}^3 = c(x)$ , imposing  $u(0) = -0.351$ ,  $u(1) = 0.597$ . Condition:  $c(x)$ ,  $x \in [0,1]$ ,  $QoI: u(x)$ ,  $x \in [0,1]$ .

### 3. Caption examples for MFC $g$ -parameter $1D \rightarrow 1D$ .

----Vague----

Investigating Mean Field Control Problem involving an interplay between density  $\rho$  and an uncertain function  $g$  inside the terminal cost. Condition:  $\rho(0,x)$ ,  $x \in [0,1]$ ,  $QoI: \rho(1,x)$ ,  $x \in [0,1]$ .

In the mean field control problem, we minimize  $\int \int \frac{1}{2} \rho^2 dx dt + \int g(x) \rho(1,x) dx$ , subject to  $\partial_t \rho + \nabla_x \cdot m = 0.02 \Delta_x \rho$ , with  $\rho(0,x) = \rho_0(x)$ , where  $g$  is an unknown function. Condition:  $\rho(0,x)$ ,  $x \in [0,1]$ ,  $QoI: \rho(1,x)$ ,  $x \in [0,1]$ .

Consider the mean field control problem with density function  $\rho(t,x)$  and terminal cost  $\int g(x) \rho(1,x) dx$  where  $g$  is an unknown function. Condition:  $\rho(0,x)$ ,  $x \in [0,1]$ ,  $QoI: \rho(1,x)$ ,  $x \in [0,1]$ .

The mean field control problem formulates  $\inf_{\rho, m} \int \int \frac{1}{2} \rho^2 dx dt + \int g(x) \rho(1,x) dx$  subject to  $\partial_t \rho + \nabla_x \cdot m = 0.02 \Delta_x \rho$ , where  $g(x)$  is undefined. Condition:  $\rho(0,x)$ ,  $x \in [0,1]$ ,  $QoI: \rho(1,x)$ ,  $x \in [0,1]$ .

----Precise----

The analysis of  $\inf_{\rho, m} \int \int \frac{1}{2} \rho^2 dx dt + \int g(x) \rho(1,x) dx$  for  $t \in [0,1]$ ,  $x \in [0,1]$  and periodic spatial boundary condition, under constraint of  $\partial_t \rho + \nabla_x \cdot m = 0.02 \Delta_x \rho$ , with the function  $g$  acting as terminal cost is defined as  $g(0), g(0.1), \dots, g(0.9) = 0.903, 0.957, 0.459, -0.178, -0.83, -1.5, -1.39, -0.189, 0.857, 0.909$ . Condition:  $\rho(0,x)$ ,  $x \in [0,1]$ ,  $QoI: \rho(1,x)$ ,  $x \in [0,1]$ .

Analyzing mean field control problem  $\inf_{\rho, m} \int \int \frac{1}{2} \rho^2 dx dt + \int g(x) \rho(1,x) dx$ , subject to the constraints, for  $t \in [0,1]$ ,  $x \in [0,1]$ , and terminal function  $g$  defined as  $g(0), g(0.1), \dots, g(0.9) = -0.244, 0.326, 0.598, 0.571, 0.287, 0.0734, 0.00921, -0.299, -0.67, -0.652$ . Condition:  $\rho(0,x)$ ,  $x \in [0,1]$ ,  $QoI: \rho(1,x)$ ,  $x \in [0,1]$ .

We solve a mean field control problem that seeks to minimize  $\inf_{\rho, m} \int \int \frac{1}{2} \rho^2 dx dt + \int g(x) \rho(1,x) dx$  while adhering to  $\partial_t \rho + \nabla_x \cdot m = 0.02 \Delta_x \rho$  and  $\rho(0,x) = \rho_0(x)$ . A known function  $g$  is given by  $g(0), g(0.1), \dots, g(0.9) = 0.535$ ,

0.976, 1.35, 1.49, 0.135, -1.86, -1.66, -0.692, -0.305, 0.0242.  
Condition:  $\rho(0, x), x \in [0, 1]$ ,  $QoI: \rho(1, x), x \in [0, 1]$

.  
Studying the mean field control problem  $\inf_{\rho, m} \iint \frac{1}{2} \rho^2 dx dt + \int g(x) \rho(1, x) dx$ , where  $t \in [0, 1], x \in [0, 1]$ , and  $g$  is given as  $g(0), g(0.1), \dots, g(0.9) = -0.0268, 0.196, 0.08, -0.0463, 0.145, 0.126, 0.169, 0.0845, -0.313, -0.413$ . Condition:  $\rho(0, x), x \in [0, 1]$ ,  $QoI: \rho(1, x), x \in [0, 1]$ .

## Details of Multi-Modal In-Context Operator Learning

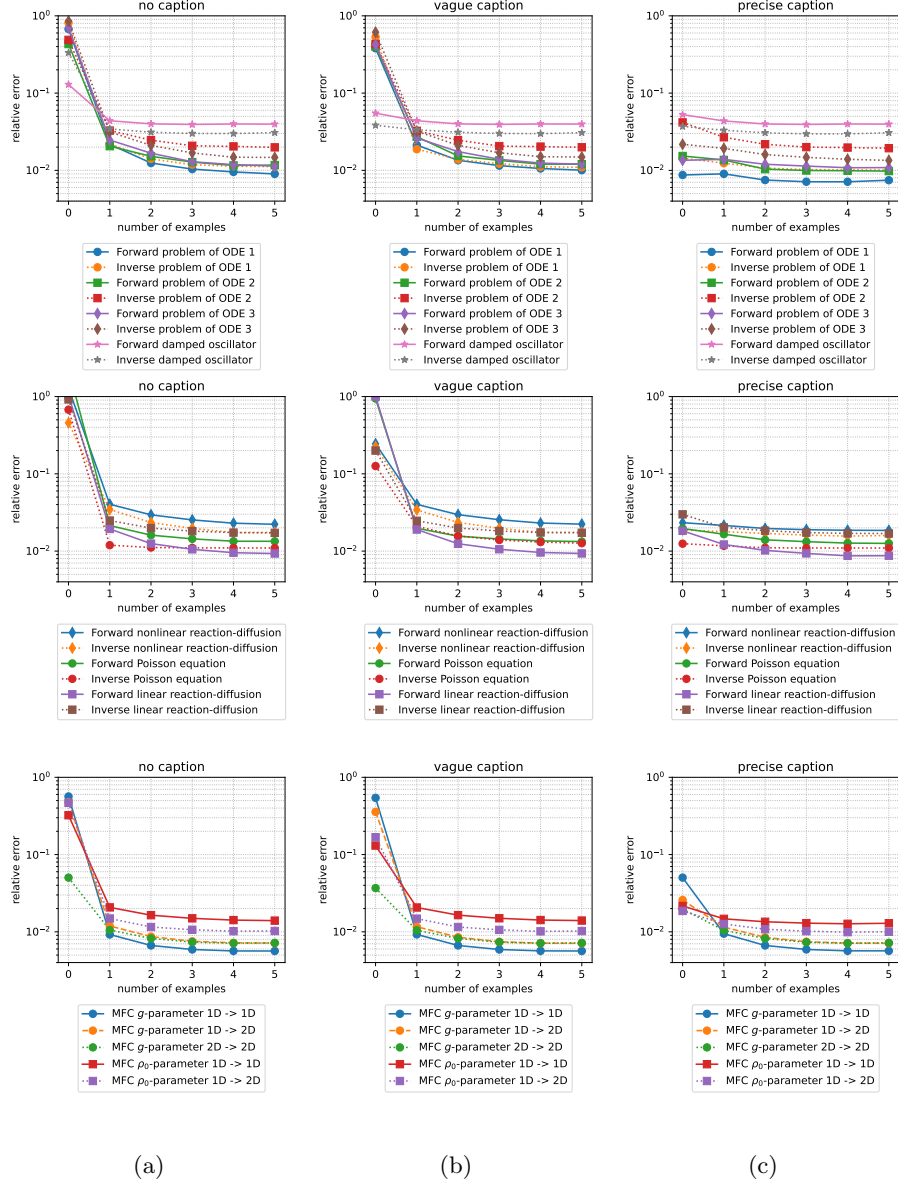


Figure 7: Relative testing error for cases from zero-shot to five-shot learning, for each type of problem. (a) Testing without captions. (b) Testing with vague captions. (c) Testing with precise captions.

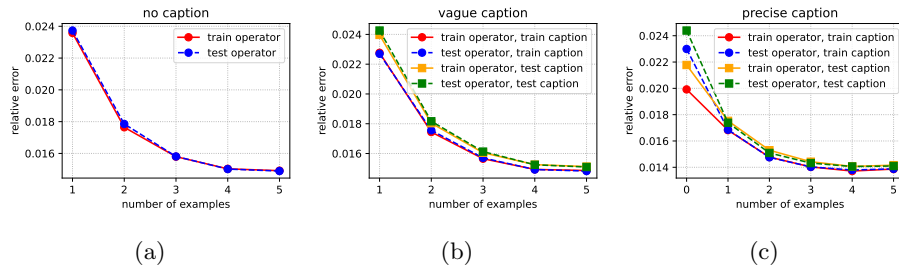


Figure 8: Relative error for cases from zero-shot to five-shot learning, using training data or testing data. (a) Learning without captions. (b) Learning with vague captions. (c) Learning with precise captions.